

# Faster Computation of Stabilizer Extent

Hiroki Hamaguchi<sup>1</sup>, Kou Hamada<sup>1</sup>, Naoki Marumo<sup>1</sup>, and Nobuyuki Yoshioka<sup>2,3,4</sup>

<sup>1</sup>Graduate School of Information Science and Technology, University of Tokyo, Tokyo, 7-3-1 Hongo, Bunkyo-ku, Tokyo 113-8656, Japan

<sup>2</sup>Department of Applied Physics, University of Tokyo, 7-3-1 Hongo, Bunkyo-ku, Tokyo 113-8656, Japan

<sup>3</sup>Theoretical Quantum Physics Laboratory, RIKEN Cluster for Pioneering Research (CPR), Wako-shi, Saitama 351-0198, Japan

<sup>4</sup>JST, PRESTO, 4-1-8 Honcho, Kawaguchi, Saitama, 332-0012, Japan

Characterization of nonstabilizerness is fruitful due to its application in gate synthesis and classical simulation. In particular, the resource monotone called the *stabilizer extent* is indispensable to estimate the simulation cost using the rank-based simulators, one of the state-of-the-art simulators of Clifford+ $T$  circuits. In this work, we propose fast numerical algorithms to compute the stabilizer extent. Our algorithm utilizes the Column Generation method, which iteratively updates the subset of pure stabilizer states used for calculation. This subset is selected based on the overlaps between all stabilizer states and a target state. Upon updating the subset, we make use of a newly proposed subroutine for calculating the *stabilizer fidelity* that (i) achieves the linear time complexity with respect to the number of stabilizer states, (ii) super-exponentially reduces the space complexity by in-place calculation, and (iii) prunes unnecessary states for the computation. As a result, our algorithm can compute the stabilizer fidelity and the stabilizer extent for Haar random pure states up to  $n = 9$  qubits, which naively requires a memory of 305 EiB. We further show that our algorithm runs even faster when the target state vector is real. The optimization problem size is reduced so that we can compute the case of  $n = 10$  qubits in 4.7 hours.

## 1 Introduction

In the domain of universal fault-tolerant quantum computation, elementary gates are often formulated to include both classically simulatable gates and more resource-intensive gates, as exemplified by the prominent Clifford+ $T$  formalism of the magic state model [1, 2, 3, 4, 5, 6]. Since Clifford circuits are classically simulatable [1], non-Clifford gates are essential for achieving quantum advantage [7, 8, 9, 10], and naturally it is crucial to improve and characterize classical simulation algorithms to quantitatively understand the computational speedups in quantum circuits [11, 12, 13, 14, 15, 16, 17, 18, 19], as well as understanding many-body phenomena in near-Clifford circuits [20, 21, 22, 23].

Hiroki Hamaguchi: [hamaguchi-hiroki0510@g.ecc.u-tokyo.ac.jp](mailto:hamaguchi-hiroki0510@g.ecc.u-tokyo.ac.jp)

Kou Hamada: [zkouaaa@g.ecc.u-tokyo.ac.jp](mailto:zkouaaa@g.ecc.u-tokyo.ac.jp)

Nobuyuki Yoshioka: [nyoshioka@ap.t.u-tokyo.ac.jp](mailto:nyoshioka@ap.t.u-tokyo.ac.jp)

When we address optimization problems involving the entire set of stabilizer states, such as the resource measures based on quasiprobability [17, 24, 25] or the stabilizer rank [11, 13, 26], the task becomes exceedingly challenging due to the super-exponential number of states involved. Among these optimization problems, the authors showed that the Robustness of Magic (RoM), formulated via Linear Program (LP), can be computed for systems up to 8 qubits by combining the Column Generation (CG) method and fast overlap calculations [27]. Naturally, this raises the question of whether the computation of the stabilizer extent, a fundamental resource measure quantifying the cost of rank-based classical simulation, can also be accelerated. However, this is not straightforward for the following reasons. (i) The problem formulation differs. While RoM exploits the density matrix of the target state, the stabilizer extent relies on the state vector. Thus, numerical techniques such as the Fast Walsh–Hadamard Transform, used in RoM computations, cannot be applied to the stabilizer extent calculation. (ii) the optimization problem is classified as a more challenging class of the Second-Order Cone Program (SOCP), reflecting that variables are complex rather than real. Due to these complications, whether the stabilizer extent can be computed for larger qubit counts has remained unclear.

In this work, we show that the above-raised issues can be solved so that the computation of the stabilizer extent can be accelerated even further than the one for the RoM. We utilize a canonical form of pure stabilizer states that allows us to enumerate them and perform fast overlap computations. We find that when we search for the subset of stabilizer states during the CG method, we can prune unnecessary states for the calculation. We numerically demonstrate that our proposed algorithm allows us to compute the stabilizer extent of a Haar random pure state up to  $n = 9$  qubits, which naively requires a memory of 305 EiB. Furthermore, with the scope of application to entanglement resource states such as GHZ or W states and eigenstates of physically meaningful Hamiltonians, we show that real-amplitude state vectors can be computed with even less computational cost. Concretely, the size of relevant stabilizer states is reduced by a factor of  $2^n$  so that we can compute the stabilizer extent of random state up to  $n = 10$  qubits.

The remainder of this paper is organized as follows. In Section 2, we present the preliminaries on the formalism of the stabilizer extent. In Section 3, we first introduce how to calculate the overlaps between all stabilizer states and a target state in Theorem 3, which serves as the main subroutine for our algorithm. Utilizing these overlap values, our proposed algorithm can compute the stabilizer extent up to 9-qubit states with drastically reduced computational resources. In Section 4, we discuss cases where the target state possesses specific properties, mainly when the state vector is real. We demonstrate that we can compute the stabilizer extent for up to 10-qubit states with real amplitudes. Finally, in Section 5, we present our findings and offer future perspectives on our work.

Table 1: The size of  $\mathcal{S}_n$ , the data size of  $A_n$  in sparse matrix format [28], and the time to compute the stabilizer extent for Haar random states by the naive method or our proposed method in Section 3.2. The last row shows the results for the case in Section 4.

n	5	6	7	8	9	10
$ \mathcal{S}_n $	2.42e+06	3.15e+08	8.13e+10	4.18e+13	4.29e+16	8.79e+19
size of $A_n$	1011 MiB	254 GiB	153 TiB	153 PiB	305 EiB	1 YiB
naive	7.7 min	×	×	×	×	×
proposed	1.4 s	2.5 s	9.2 s	4.3 min	7.7 h	×
real case	0.5 s	0.5 s	3.5 s	14.7 s	6.9 min	4.7 h

## 2 Preliminaries

Let  $\mathcal{S}_n := \{|\phi_j\rangle\}$  be the entire set of  $n$ -qubit stabilizer states. Let  $\sigma_j := |\phi_j\rangle\langle\phi_j|$  denote the density matrix for  $|\phi_j\rangle$ . The size of  $\mathcal{S}_n$  scales super-exponentially as  $|\mathcal{S}_n| = 2^n \prod_{k=0}^{n-1} (2^{n-k} + 1) = 2^{\mathcal{O}(n^2)}$  [29, Proposition 1]. See also Table 1 for the size of  $\mathcal{S}_n$ .

It is informative to provide the definition of the *Robustness of Magic* (RoM), which quantifies the nonstabilizerness of an  $n$ -qubit mixed state  $\rho$  as follows [30]:

$$\mathcal{R}(\rho) := \min_{c \in \mathbb{R}^{|\mathcal{S}_n|}} \left\{ \|c\|_1 \mid \rho = \sum_{j=1}^{|\mathcal{S}_n|} c_j \sigma_j \right\}.$$

On the other hand, the *stabilizer extent* quantifies an  $n$ -qubit pure state  $|\psi\rangle$  as follows [31, Definition 3]:

$$\xi(\psi) := \min_{c \in \mathbb{C}^{|\mathcal{S}_n|}} \left\{ \|c\|_1^2 \mid |\psi\rangle = \sum_{j=1}^{|\mathcal{S}_n|} c_j |\phi_j\rangle \right\}. \quad (1)$$

This definition can be simplified as the complex  $L^1$ -norm minimization problem as follows:

$$\sqrt{\xi(\psi)} = \min_{x \in \mathbb{C}^{|\mathcal{S}_n|}} \{ \|x\|_1 \mid A_n x = b \}, \quad (2)$$

where  $A_n \in \mathbb{C}^{2^n \times |\mathcal{S}_n|}$  is defined as  $(A_n)_{i,j} := \langle i | \phi_j \rangle$  and  $b \in \mathbb{C}^{2^n}$  as  $b_i := \langle i | \psi \rangle$  using the computational basis  $\{|i\rangle\}_{i=0}^{2^n-1}$ . The problem (2) is pointed out to be a Second-Order Cone Program (SOCP) [26], and thus by defining  $\mathcal{A}_n$  as the columns set  $\{a_j\}$  of  $A_n$ , its dual problem can be derived as [26, Appendix A][32, Section 5.1.6]

$$\sqrt{\xi(\psi)} = \max_{y \in \mathbb{C}^{2^n}} \left\{ \operatorname{Re}(b^\dagger y) \mid |a_j^\dagger y| \leq 1 \text{ for all } a_j \in \mathcal{A}_n \right\}, \quad (3)$$

where  $\dagger$  denotes the conjugate transpose, or in the case of a scalar, the complex conjugate.

Further, we introduce a function  $\text{SolveSOCP}(\mathcal{C}, b)$  to describe our algorithm in later sections with the symbol  $\mathcal{C} \subseteq \mathcal{A}_n$  representing a column subset. The function solves a problem that can be obtained by restricting  $\mathcal{A}_n$  to  $\mathcal{C}$ , and returns the solution  $x$  for the corresponding restricted primal problem of (2) as well as the solution  $y$  for the restricted dual problem of (3). In the actual implementation, this function can be realized by just solving the primal problem with SOCP solver, such as MOSEK [33] or CVXPY [34, 35].

## 3 Scaling Up the Exact Stabilizer Extent Calculation

Although both the RoM and the stabilizer extent are quantifiable through convex optimization problems, it is impractical to solve them naively for  $n > 5$  qubit systems due to the super-exponential growth of the number of stabilizer states  $|\mathcal{S}_n|$ , as shown in Table 1. Moreover, to formulate the problem in the standard form, we need at least twice the memory size of  $A_n$ . For the case of RoM calculation, the authors proposed to employ a classical optimization technique known as the Column Generation (CG) method [27]. However, it is nontrivial whether the same approach could be applied to other resource measures since the structure of the matrix  $A_n$  used for the calculation is heavily dependent on the measures. For the stabilizer extent, in particular, the SOCP is known to be a strict extension of the LP, and hence more difficult to solve in general [32, Section 4.4.2].

In the following, we fill in these gaps by utilizing the specific structure of stabilizer states. We first introduce a crucial subroutine for fast overlap calculation in Sec. 5 which reduces the size of  $A_n$  via the branch and bound method [36], and then show how the computation can be scaled up by utilizing the CG method in Sec. 3.2.

### 3.1 Core Subroutine: Calculating Stabilizer Fidelity

To utilize the CG method, we first propose a subroutine to compute the *stabilizer fidelity* introduced in Ref. [13], which is the maximal overlap between the target state and all the stabilizer states. For a pure quantum state  $|\psi\rangle$  the stabilizer fidelity is defined as follows:

$$\sqrt{F(\psi)} := \max_{\phi \in \mathcal{S}_n} |\langle \phi | \psi \rangle| = \max_{a_j \in \mathcal{A}_n} |a_j^\dagger b|.$$

Note that the extension of stabilizer fidelity to mixed states has been pointed out as essential for the fast computation of RoM [27]. As expected from the direct relationships between the stabilizer fidelity and the stabilizer extent [26][31, Proposition 2], we find the stabilizer fidelity  $F$  is also crucial for the computation of the stabilizer extent  $\xi$ .

In the following, we present how to compute the stabilizer fidelity up to 9-qubit systems. To this end, we first introduce the following theorem, which is useful for enumerating all the stabilizer states. This theorem is a variant of previous work [37, Theorem 2][38, Section 5][39, Theorem 5.(ii)]. The proof is given in Appendix A.1.

**Theorem 1.** *Let  $\mathbb{F}_2$  be the finite field with two elements. For all  $k \in \{1, \dots, n\}$ , we define*

$$\begin{aligned} \mathcal{Q}_k &:= \left\{ Q \mid Q \in \mathbb{F}_2^{k \times k} \text{ is an upper triangular matrix} \right\}, \\ \mathcal{R}_k &:= \left\{ R \mid R \in \mathbb{F}_2^{n \times k} \text{ is a reduced column echelon form matrix with } \text{rank}(R) = k \right\}, \\ \mathcal{T}_R &:= \left\{ t \mid t \in \mathbb{F}_2^n \text{ is a representative of element in the quotient space } \mathbb{F}_2^n / \text{Im}(R) \right\}. \end{aligned}$$

We also define the set of states  $\mathcal{S}_{n,k}$  as

$$\mathcal{S}_{n,k} := \left\{ \frac{1}{2^{k/2}} \sum_{x=0}^{2^k-1} (-1)^{x^\top Q x} i^{c^\top x} |Rx + t\rangle \mid Q \in \mathcal{Q}_k, c \in \mathbb{F}_2^k, R \in \mathcal{R}_k, t \in \mathcal{T}_R \right\}, \quad (4)$$

and define  $\mathcal{S}_{n,0} := \{|t\rangle \mid t \in \mathbb{F}_2^n\}$ . Then, we have  $\bigcup_{k=0}^n \mathcal{S}_{n,k} = \mathcal{S}_n$ .

Here, we identify a integer  $\sum_{i=0}^{n-1} x_i 2^i$  with a vector  $[x_0 \ x_1 \ \dots \ x_{n-1}]^\top$ . Let  $|\phi\rangle$  be one of the stabilizer states with  $k > 0$  in Theorem 1,  $|\phi\rangle = \frac{1}{2^{k/2}} \sum_{x=0}^{2^k-1} (-1)^{x^\top Q x} i^{c^\top x} |Rx + t\rangle$ . Then, by denoting  $a \in \mathcal{A}_n$  as the corresponding state vector of  $|\phi\rangle$ , the overlap between  $|\psi\rangle$  and  $|\phi\rangle$  is given by  $a^\dagger b = \sum_{i=0}^{2^n-1} \langle \phi | i \rangle \langle i | \psi \rangle = \langle \phi | \psi \rangle$  and

$$|\langle \phi | \psi \rangle| = \left| \frac{1}{2^{k/2}} \sum_{x=0}^{2^k-1} \left( (-1)^{x^\top Q x} i^{c^\top x} \right)^\dagger \langle Rx + t | \psi \rangle \right| = \left| \sum_{x=0}^{2^k-1} (-1)^{x^\top Q x} i^{c^\top x} \left( \frac{1}{2^{k/2}} b_{Rx+t}^\dagger \right) \right|.$$

In the following, we define  $P_x := \frac{1}{2^{k/2}} b_x^\dagger$ . For simplicity, we fix  $k = n, R = I_n, t = 0$ . This assumption can be made without loss of generality, and the other cases can be easily reduced to this case. Recall that our goal is to compute  $\max_{a_j \in \mathcal{A}_n} |a_j^\dagger b|$ . Owing to the equation above, this is equivalent to the following problem except for the case  $k = 0$ :

$$\max_{Q,c} \left\{ \left| \sum_{x=0}^{2^n-1} (-1)^{x^\top Q x} i^{c^\top x} P_x \right| \right\}. \quad (5)$$

If we solve (5) naively, the time complexity is  $\mathcal{O}\left(2^{n+n(n+1)/2} 2^n n^2\right)$ , where  $2^{n+n(n+1)/2}$  is the number of combinations for  $(Q, c)$ ,  $2^n$  is the number of the terms in the summation, and  $n^2$  is the computational cost per each term. However, we find that we can solve the problem much faster:

**Theorem 2.** *Problem (5) can be solved with the time complexity of  $\mathcal{O}(2^{n+n(n+1)/2})$  and the space complexity of  $\mathcal{O}(2^n)$ .*

*Proof.* We first show that we can substitute  $\mathbb{F}_2$  with  $\{0, 1\} \subset \mathbb{Z}$  for the elements of  $Q$  and  $c$ . This indicates that  $i^{\alpha+\beta} = i^\alpha i^\beta$  holds true, whereas in  $\mathbb{F}_2$  it does not hold since  $-1 = i^{1+1} \neq i^0 = 1$  for  $1+1=0$ . By this substitution, the term  $(-1)^{x^\top Q x}$  is invariant, while the term  $i^{c^\top x}$  is multiplied by  $-1$  if and only if  $p \equiv 2, 3 \pmod{4}$ , where  $p$  is the number of  $i$  such that  $c_i = 1$  and  $x_i = 1$ . Now, for  $k > 0$  we consider  $|\phi\rangle = \frac{1}{2^{k/2}} \sum_{x=0}^{2^k-1} (-1)^{x^\top (Q+Q')x} i^{c^\top x} |Rx + t\rangle$  where  $Q'_{i,j} = 1 \iff (i < j) \wedge (c_i = c_j = 1)$ . If the pair  $(Q, c, R, t)$  in this expression is the same as that of the original form (4), then the two states represent the same state since

$$(-1)^{x^\top Q' x} = (-1)^{\binom{p}{2}} = \begin{cases} 1 & \text{if } p \equiv 0, 1 \pmod{4}, \\ -1 & \text{if } p \equiv 2, 3 \pmod{4}. \end{cases}$$

By identifying  $Q+Q' \in \mathbb{Z}^{k \times k}$  with  $Q \in \mathbb{F}_2^{k \times k}$ , we indeed find that the substitution is valid.

Let us solve the problem (5). The case  $n = 1$  is obvious. For  $n > 1$ , we define

$$Q := \begin{bmatrix} Q_{00} & Q_0^\top \\ 0 & \bar{Q} \end{bmatrix} \left( Q_{00} \in \{0, 1\}, Q_0 \in \{0, 1\}^{n-1}, \bar{Q} \in \{0, 1\}^{(n-1) \times (n-1)} \right),$$

$$c := \begin{bmatrix} c_0 \\ \bar{c} \end{bmatrix} \left( c_0 \in \{0, 1\}, \bar{c} \in \{0, 1\}^{n-1} \right), \quad x := \begin{bmatrix} x_0 \\ \bar{x} \end{bmatrix} \left( x_0 \in \{0, 1\}, \bar{x} \in \{0, 1\}^{n-1} \right).$$

Since  $x^\top Q x = x_0(Q_{00} + Q_0^\top \bar{x}) + \bar{x}^\top \bar{Q} \bar{x}$  and  $c^\top x = c_0 x_0 + \bar{c}^\top \bar{x}$ , we can derive that

$$\begin{aligned} \sum_{x=0}^{2^n-1} (-1)^{x^\top Q x} i^{c^\top x} P_x &= \sum_{\bar{x}=0}^{2^{n-1}-1} (-1)^{\bar{x}^\top \bar{Q} \bar{x}} i^{\bar{c}^\top \bar{x}} \left( P_{2\bar{x}} + (-1)^{Q_{00}+Q_0^\top \bar{x} c_0} P_{2\bar{x}+1} \right) \\ &= \sum_{\bar{x}=0}^{2^{n-1}-1} (-1)^{\bar{x}^\top \bar{Q} \bar{x}} i^{\bar{c}^\top \bar{x}} \bar{P}_{\bar{x}} \end{aligned} \quad (6)$$

where  $\bar{P}_{\bar{x}} := P_{2\bar{x}} + (-1)^{Q_{00}+Q_0^\top \bar{x} c_0} P_{2\bar{x}+1}$ . Since (6) is the same form as the original one, the problem (5) can be solved recursively by fixing the value  $Q_{00}, Q_0$  and  $c_0$ .

We now analyze the time complexity of this recursive algorithm. There are  $2^{n+1}$  possible combinations of  $Q_{00}, Q_0$ , and  $c_0$ . For each combination,  $\bar{P}_{\bar{x}}$  can be computed in  $\mathcal{O}(n2^{n-1})$  time. Hence, we can establish the recurrence relation for the time complexity:

$$T(n) = 2^{n+1}(n2^{n-1} + T(n-1)), \quad T(1) = 4.$$

Solving this recurrence relation yields

$$T(n) = 2^{n+\frac{n(n+1)}{2}} + \sum_{d=2}^n 2^{n+\frac{n(n+1)}{2}-\frac{d(d-1)}{2}} d,$$

$$\frac{T(n)}{2^{n+\frac{n(n+1)}{2}}} = 1 + \sum_{d=2}^n 2^{-\frac{d(d-1)}{2}} d \leq 1 + \sum_{d=2}^n 2^{-d+1} d = 4 - (n+2)2^{-n+1} \rightarrow 4 \quad (n \rightarrow \infty).$$

Therefore, the time complexity is  $\mathcal{O}(2^{n+n(n+1)/2})$ . Doing this recursive algorithm through in-place computation establishes the space complexity of  $\mathcal{O}(2^n)$  (see also Fig. 1).  $\square$

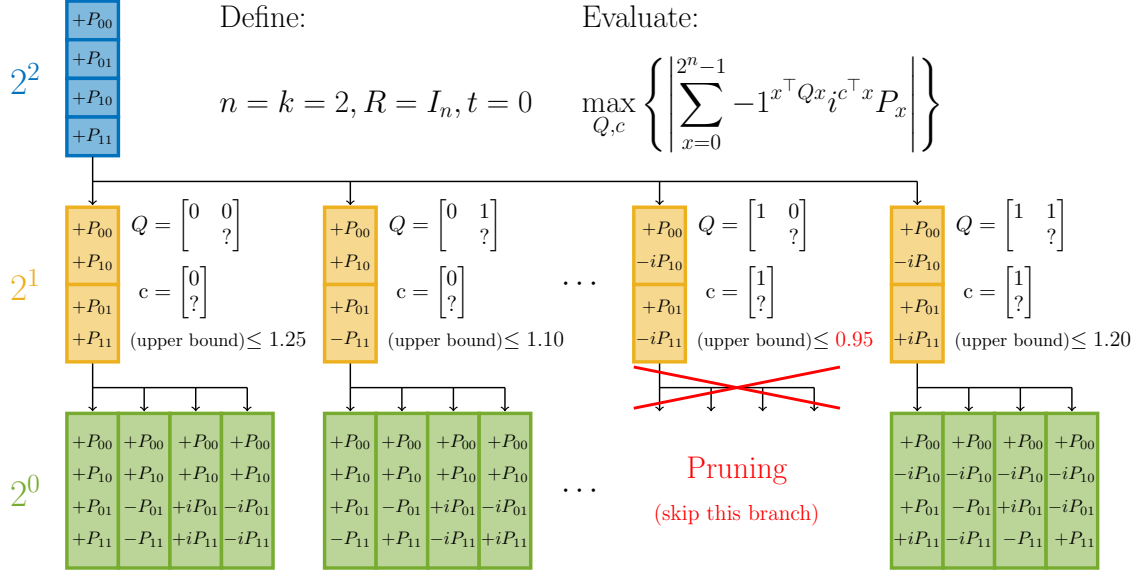


Figure 1: Visualization of stabilizer pruning. Each cell stores the evaluated value of the expression, and the  $2^{n+n(n+1)/2}$  leaf nodes correspond to the value  $\sum_{x=0}^{2^n-1} (-1)^{x^\top Q x} i^{c^\top x} P_x$ . Since we only need one set of cells per color during the procedure, we can do it in place. This means the space complexity is  $\mathcal{O}(\sum_{i=0}^n 2^i)$ , i.e.,  $\mathcal{O}(2^n)$ .

Note that the actual implementation of the recursive computation is done in a slightly modified way to improve efficiency. See our GitHub repository [40] for the codes, including the enumeration of the stabilizer states based on Theorem 1. Moreover, we can further enhance the efficiency by employing branch-cut heuristics which we describe in detail below.

We call the proposed algorithm to compute the stabilizer fidelity as *stabilizer pruning*, which is based on Theorem 2 and the branch and bound method [36] (see Fig. 1 for its visual representation). The main idea is that, since we are solving a maximization problem, solutions inferior to the current best solution (or to 1 for the case in Section 3.2.2) are unnecessary. We can thus terminate branching if the upper bound of the current state is lower than these values. For more details on the pruning strategy, see Appendix A.2. By applying a similar argument for every  $k, R$ , and  $t$ , we can derive the next theorem.

**Theorem 3.** *The stabilizer fidelity of a  $n$ -qubit pure state  $|\psi\rangle$  can be computed in the time complexity of  $\mathcal{O}(|S_n|)$  and the space complexity of  $\mathcal{O}(2^n)$ .*

Let us briefly discuss the numerical results of the stabilizer pruning. We find that the run time to compute the stabilizer fidelity of a Haar random 8-qubit state is 5 seconds, and that of a 9-qubit state is 26 minutes. We will use a slightly modified version of this algorithm as a subroutine to compute the stabilizer extent; namely, besides finding the maximum, we also identify other large overlaps. All numerical experiments in this paper were conducted using C++17 compiled by GCC 9.4.0 and a cluster computer powered by Intel(R) Xeon(R) CPU E52640 v4 with 270 GB of RAM using 40 threads. All the codes are available at GitHub [40].

### 3.2 CG Method for Stabilizer Extent Calculation

Next, we introduce the Column Generation (CG) method [41], the primary method to compute the stabilizer extent  $\xi(\psi)$  up to 9-qubit systems. Our proposed algorithm with

the CG method, as outlined in Algorithm 1, is an iterative algorithm that solves a sub-problem restricted to  $\mathcal{C} \subseteq \mathcal{A}_n$  per iteration. It initializes a small subset of columns  $\mathcal{C}_0$  and updates it so that the number of violated constraints reduces until there are no more violated columns. The execution time of this algorithm for a Haar random state is described in Table 1. While we direct the readers to Ref. [27] for further implementation techniques, we describe two critical aspects of this algorithm: the initialization process and the solution’s optimality.

---

**Algorithm 1:** Exact Stabilizer Extent Calculation by Column Generation

---

**Input:** Vector  $b \in \mathbb{C}^{2^n}$  corresponding to the state  $|\psi\rangle$   
**Output:** Exact stabilizer extent  $\xi(\psi)$

```

1  $\mathcal{C}_0 \leftarrow$  Partial set of  $\mathcal{A}_n$            /* Initialize using top overlap  $|a_j^\dagger b|$  */
2 for  $k = 0, 1, 2, \dots$  do
3    $x_k, y_k \leftarrow \text{SolveSOCP}(\mathcal{C}_k, \mathbf{b})$ 
4    $\hat{\xi}_k(\psi) \leftarrow \|x_k\|_1^2$ 
5    $\mathcal{C}' \leftarrow \{a_j \in \mathcal{A}_n \mid |a_j^\dagger y_k| > 1\}$  /* Use of subroutine in Section 3.1 */
6   if  $\mathcal{C}' = \emptyset$  then
7     return  $\xi(\psi) = \hat{\xi}_k(\psi)$ 
8    $\mathcal{C}_{k+1} \leftarrow \mathcal{C}_k \cup \mathcal{C}'$ 

```

---

### 3.2.1 Initialization

We find that the quality of the initial guess and the number of optimization steps of Algorithm 1 can be significantly improved by choosing a subset  $\mathcal{C}_0 \subseteq \mathcal{A}_n$  in descending order of  $|a_j^\dagger b|$ , which can be computed with the complexity as stated in Theorem 3. While the size of  $\mathcal{C}_0$  is arbitrary, in computations in Table 1, we have chosen the size to be 10,000 for  $n \leq 8$  and 100,000 for  $n = 9$ .

The use of  $|a_j^\dagger b| = |\langle \phi_j | \psi \rangle|$  as the indicator can be justified with various interpretations. One of them is to consider it as the “closeness” between the states  $|\phi_j\rangle$  and  $|\psi\rangle$ , which means choosing states based on their overlaps is reasonable. The numerical experiment result in Fig. 2 also supports the effectiveness of this indicator. For a Haar random pure 8-qubit state, even if we use as small a subset as  $|\mathcal{C}_0| = 10^{-10}|\mathcal{A}_n|$ , the obtained value  $\hat{\xi}_0(\psi)$  closely approximated the exact value  $\xi(\psi)$  and outperformed randomly selected  $\mathcal{C}_0$ . Such behavior was typical in other test cases, including 9-qubit states.

### 3.2.2 Solution’s optimality

The terminate criterion for Algorithm 1 is the absence of columns that violate the dual constraints  $|a_j^\dagger y_k| \leq 1$ , able to check by Theorem 3 as well. The termination of the CG method indicates that the optimal dual solution for problem (3) has been found, which then implies that the primal solution  $x_k$  is also optimal for problem (2), due to the strong duality of the SOCP. Consequently, we can affirm that Algorithm 1 will compute the stabilizer extent for any state  $|\psi\rangle$  once it terminates. The convergence of the CG method was further validated through numerical experiments. For the same 8-qubit state,  $\max_{a_j \in \mathcal{A}_n} |a_j^\dagger y_k|$  reached unity after 4 iterations, indicating the discovery of the optimal solution. The method converged within just 1 or 2 iterations for different test cases.

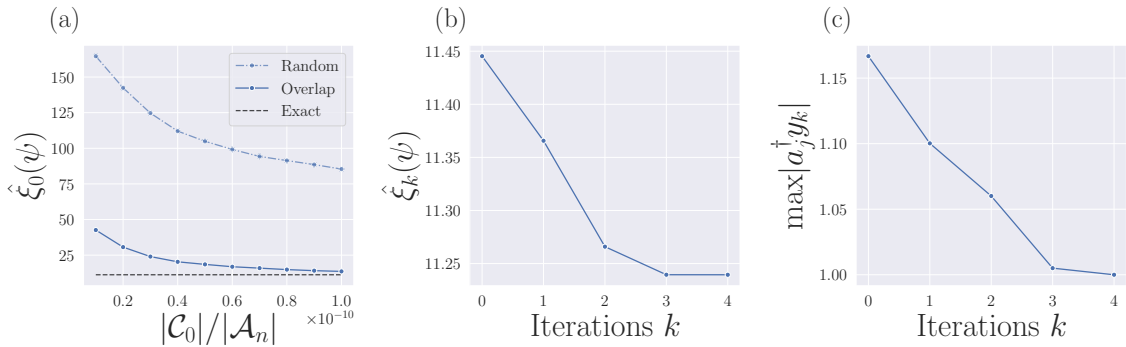


Figure 2: (a) Provisional value  $\hat{\xi}_0(\psi)$  in the Algorithm 1 for a Haar random 8-qubit state. The ratio  $|\mathcal{C}_0|/|\mathcal{A}_n|$  varies from  $10^{-11}$  to  $10^{-10}$ . We got much better results with the top overlap method compared to the randomly selected  $\mathcal{C}_0$ . The black dotted line labeled as “Exact” represents  $\xi(\psi)$ . (b) The convergence of the CG method for the same state. (c)  $\max_{a_j \in \mathcal{A}_n} |a_j^\dagger y_k|$  reached 1.00 after 4 iterations, indicating that the optimal solution had been found. The time for this computation was 4.3 minutes.

## 4 Calculation for States With Special Properties

So far, we have explored the method for calculating the stabilizer extent applicable to the general case up to  $n \leq 9$ . While the super-exponential growth of  $|\mathcal{S}_n|$  is prohibitive, the computation can be further extended to a larger size when the target state is classified into specific classes.

One such example is a product state,  $|\psi\rangle = \bigotimes_j |\psi_j\rangle$ . It is known that if all the components  $|\psi_j\rangle$  are at most 3-qubit state, then the multiplicativity holds as  $\xi(\psi) = \prod_j \xi(\psi_j)$  [31]. While we cannot guarantee the multiplicativity if the factors contain a 4 or more qubits state [26], the tensor product of each solution  $x_j$  of  $\xi(\psi_j)$  is still practically useful since it can be used as the initial guess for the solution of  $\xi(\psi)$ .

Another remarkable class of states is those with real amplitudes. To the best of our knowledge, this property has not been investigated in previous works and offers significant calculation advantages. One of the well-known examples is the W-state and the GHZ-state, defined as follows:

$$|W\rangle := \frac{1}{\sqrt{n}}(|100\dots 0\rangle + |010\dots 0\rangle + \dots + |000\dots 1\rangle), \quad |GHZ\rangle := \frac{|0\rangle^{\otimes n} + |1\rangle^{\otimes n}}{\sqrt{2}}.$$

Other critical applications include eigenstates of quantum many-body Hamiltonians with time-reversal symmetry, whose matrix elements are given by real components. For instance, physically meaningful Hamiltonians such as in XXZ and Heisenberg spin models, transverse-field Ising model, Fermi–Hubbard model, and  $t$ - $J$  model all preserve the time-reversal symmetry regardless of the underlying lattice. Beyond condensed matter systems, we may also consider first-principle quantum chemistry Hamiltonians or lattice gauge theory Hamiltonians such as the 1d Schwinger model. Note that the abundance of examples reflects that the microscopic equation of motion is time-reversal symmetric unless there is a spontaneous symmetry breaking or the weak interaction.

We envision that other symmetries contribute to accelerating the computation while we leave the study of general symmetry to be an open question.



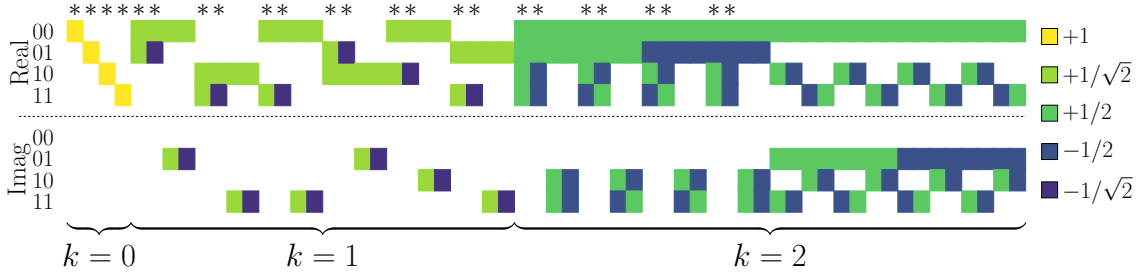


Figure 3: Visualization of the matrix  $A_n$ , i.e., the column set  $\mathcal{A}_n$ , with  $n = 2$ . The upper half corresponds to the real part, and the lower half corresponds to the imaginary part. The  $j$ -th column of this represents the state vector  $a_j$  of the stabilizer state  $|\phi_j\rangle$ . The integer  $k$  below the matrix corresponds to the integer  $k$  in Theorem 1. By restricting the column set  $\mathcal{A}_n$  to the starred columns, which are real vectors, we can obtain  $\mathcal{A}'_n$ .

#### 4.1 Reduction of Problem Size in Real-amplitude States

In the following, we argue that the stabilizer extent for real-amplitude states can be computed significantly faster than complex-amplitude ones, with a numerical demonstration for uniformly random quantum states with real amplitudes up to 10-qubit systems. Targeting random states allows us to avoid assuming unnecessary specificity, thereby demonstrating the broad computational potential.

Firstly, we define  $\mathcal{S}'_n \subset \mathcal{S}_n$  as follows:

$$\mathcal{S}'_n = \{|\phi_j\rangle \in \mathcal{S}_n \mid \langle i|\phi_j\rangle \in \mathbb{R} \text{ for all } i\}.$$

This means that  $\mathcal{S}'_n$  is the union of  $\mathcal{S}_{n,0}$  and the set of states with  $c = 0$  in Theorem 1. Let  $\mathcal{A}'_n$  denote the corresponding subset of the columns in  $\mathcal{A}_n$ . Also refer to Fig. 3 for the definition of  $\mathcal{A}'_n$ . Then, the next lemma holds.

**Lemma 1.** *For a state  $|\psi\rangle$ , suppose its state vector  $b$  is real. Then, we have*

$$\max_{a \in \mathcal{A}_n} |a^\dagger b| = \max_{a \in \mathcal{A}'_n} |a^\dagger b|.$$

*Proof.* We only show  $\max_{a \in \mathcal{A}_n} |a^\dagger b| \leq \max_{a \in \mathcal{A}'_n} |a^\dagger b|$  since  $\mathcal{A}_n \supset \mathcal{A}'_n$ . Fix  $a \in \mathcal{A}_n \setminus \mathcal{A}'_n$ . Since  $a \notin \mathcal{A}'_n$ ,  $k > 0$  in the form of Theorem 1 and  $|\phi\rangle = \frac{1}{2^{k/2}} \sum_{x=0}^{2^k-1} (-1)^{x^\top Qx} i^{c^\top x} |Rx + t\rangle$ . Suppose  $a^\dagger y = \alpha + i\beta$  ( $\alpha, \beta \in \mathbb{R}$ ). The following two states

$$|\phi_+\rangle := \frac{1}{2^{k/2}} \sum_{x=0}^{2^k-1} (-1)^{x^\top Qx} |Rx + t\rangle, \quad |\phi_-\rangle := \frac{1}{2^{k/2}} \sum_{x=0}^{2^k-1} (-1)^{x^\top Qx + c^\top x} |Rx + t\rangle$$

only have real amplitudes and belong to  $\mathcal{S}'_n$ . Define  $a_+$  and  $a_-$  as the vectors in  $\mathcal{A}'_n$  of  $|\phi_+\rangle$  and  $|\phi_-\rangle$ , respectively. Since  $c \in \mathbb{F}_2^k$ , we have  $a_+^\dagger y = \alpha + \beta$ ,  $a_-^\dagger y = \alpha - \beta$ , and

$$|a^\dagger b| = \sqrt{\alpha^2 + \beta^2} \leq |\alpha| + |\beta| = \max\{|\alpha + \beta|, |\alpha - \beta|\} \leq \max_{a \in \mathcal{A}'_n} |a^\dagger b|.$$

This completes the proof.  $\square$

We can derive the following corollary by combining Lemma 1 and Theorem 3.

**Corollary 1.** *The stabilizer fidelity of a  $n$ -qubit state  $|\psi\rangle$  with real amplitudes can be computed in time complexity of  $\mathcal{O}(|\mathcal{S}_n|/2^n)$  and space complexity of  $\mathcal{O}(2^n)$ .*

Now, we can prove the following theorem by Lemma 1.

**Theorem 4.** *Suppose that  $|\psi\rangle$  is a state with real amplitudes. The optimal solution for the restricted problem (3) where  $\mathcal{A}_n$  is substituted by  $\mathcal{A}'_n$  is also optimal for the original problem (3).*

*Proof.* Let  $x^*$  and  $y^*$  be the optimal solutions of the restricted primal and dual problems, namely, problems (2) and (3) with  $\mathcal{A}'_n$  instead of  $\mathcal{A}_n$ . We can ensure that such solutions always exist. Define  $x^{**}$  as

$$x_j^{**} = \begin{cases} x_j^* & \text{if } a_j \in \mathcal{A}'_n, \\ 0 & \text{if } a_j \notin \mathcal{A}'_n. \end{cases}$$

We will show that  $x^{**}$  and  $y^*$  are optimal solutions for the original problems.

Let OPT be the optimal value for the original problems. Since  $x^{**}$  is a feasible solution for the original primal problem, it is clear that  $\text{OPT} \leq \|x^{**}\|_1 = \|x^*\|_1$ . By the strong duality theorem, OPT is also the optimal value for the original dual problem. From Lemma 1, we know that  $y^*$  is not only a feasible solution for the restricted dual problem but also for the original dual problem, hence  $\text{OPT} \geq \text{Re}(b^\dagger y^*)$ . Again, by applying the strong duality theorem to the restricted problems, we obtain  $\|x^*\|_1 = \text{Re}(b^\dagger y^*)$ , which implies that  $\text{OPT} = \|x^{**}\|_1 = \text{Re}(b^\dagger y^*)$ . Therefore,  $x^{**}$  and  $y^*$  are also optimal solutions for the original problems.  $\square$

Thanks to Theorem 4, we can reduce the size of the column set size by a factor of  $2^n$ . We also conducted a numerical experiment for a uniformly random 10-qubit state with real amplitudes. The algorithm converged within a single iteration using  $|\mathcal{C}_0| = 100,000$  as in Section 3.2.1, which was sufficiently large to obtain the stabilizer extent. This result confirmed our success in computing its stabilizer extent, accomplished within a time frame of 4.7 hours.

## 5 Discussion

In this paper, we have shown that the stabilizer fidelity and the stabilizer extent can be calculated by utilizing the specific structure of stabilizer states. We proposed an algorithm based on the branch and bound method and the CG method to compute the exact stabilizer extent and demonstrated its applicability to sufficiently large systems. Additionally, we proposed a specialized algorithm for states with real amplitudes.

While the idea of applying resource theory to quantum computing has attracted a significant amount of interest, the barrier of computational hardness (in particular, memory consumption) has prevented us from gaining further benefits for circuit design and optimization. We envision that the methodology proposed in this work shall not be limited to the stabilizer extent but also expected to generalize to other monotones such as the dyadic negativity [17].

## Acknowledgments

We thank Shigeo Hakkaku, Bartosz Regula, and Ryuji Takagi for their helpful discussions. N.Y. wishes to thank JST PRESTO No. JPMJPR2119 and the support from IBM Quantum. This work was supported by JST Grant Number JPMJPF2221. This work was supported by JST ERATO Grant Number JPMJER2302 and JST CREST Grant Number JPMJCR23I4, Japan.

## References

- [1] Daniel Gottesman. “The Heisenberg Representation of Quantum Computers” (1998). [arxiv:quant-ph/9807006](#).
- [2] Michael A. Nielsen and Isaac L. Chuang. “Quantum Computation and Quantum Information: 10th Anniversary Edition”. [Cambridge University Press](#). (2010).
- [3] Sergei Bravyi and Alexei Kitaev. “Universal Quantum Computation with ideal Clifford gates and noisy ancillas”. [Physical Review A](#) **71**, 022316 (2005).
- [4] Daniel Litinski. “A Game of Surface Codes: Large-Scale Quantum Computing with Lattice Surgery”. [Quantum](#) **3**, 128 (2019).
- [5] Dominic Horsman, Austin G Fowler, Simon Devitt, and Rodney Van Meter. “Surface code quantum computing by lattice surgery”. [New Journal of Physics](#) **14**, 123011 (2012).
- [6] Austin G. Fowler and Craig Gidney. “Low overhead quantum computation using lattice surgery” (2019). [arxiv:1808.06709](#).
- [7] Craig Gidney and Martin Ekerå. “How to factor 2048 bit RSA integers in 8 hours using 20 million noisy qubits”. [Quantum](#) **5**, 433 (2021).
- [8] Joonho Lee, Dominic W. Berry, Craig Gidney, William J. Huggins, Jarrod R. McClean, Nathan Wiebe, and Ryan Babbush. “Even More Efficient Quantum Computations of Chemistry Through Tensor Hypercontraction”. [PRX Quantum](#) **2**, 030305 (2021).
- [9] Vera von Burg, Guang Hao Low, Thomas Häner, Damian S. Steiger, Markus Reiher, Martin Roetteler, and Matthias Troyer. “Quantum computing enhanced computational catalysis”. [Physical Review Research](#) **3**, 033055 (2021).
- [10] Nobuyuki Yoshioka, Tsuyoshi Okubo, Yasunari Suzuki, Yuki Koizumi, and Wataru Mizukami. “Hunting for quantum-classical crossover in condensed matter problems”. [npj Quantum Information](#) **10**, 45 (2024).
- [11] Sergey Bravyi, Graeme Smith, and John Smolin. “Trading classical and quantum computational resources”. [Physical Review X](#) **6**, 021043 (2016).
- [12] Sergey Bravyi and David Gosset. “Improved Classical Simulation of Quantum Circuits Dominated by Clifford Gates”. [Physical Review Letters](#) **116**, 250501 (2016).
- [13] Sergey Bravyi, Dan Browne, Padraic Calpin, Earl Campbell, David Gosset, and Mark Howard. “Simulation of quantum circuits by low-rank stabilizer decompositions”. [Quantum](#) **3**, 181 (2019).
- [14] Emanuele Tirrito, Poetri Sonya Tarabunga, Guglielmo Lami, Titas Chanda, Lorenzo Leone, Salvatore F. E. Oliviero, Marcello Dalmonte, Mario Collura, and Alioscia Hama. “Quantifying nonstabilizerness through entanglement spectrum flatness”. [Physical Review A: Atomic, Molecular, and Optical Physics](#) **109**, L040401 (2024).
- [15] Oliver Hahn, Alessandro Ferraro, Lina Hultquist, Giulia Ferrini, and Laura García-Álvarez. “Quantifying Qubit Magic Resource with Gottesman-Kitaev-Preskill Encoding”. [Physical Review Letters](#) **128**, 210502 (2022).
- [16] Tobias Haug, Soovin Lee, and M. S. Kim. “Efficient quantum algorithms for stabilizer entropies” (2023). [arxiv:2305.19152](#).
- [17] James R. Seddon, Bartosz Regula, Hakop Pashayan, Yingkai Ouyang, and Earl T. Campbell. “Quantifying Quantum Speedups: Improved Classical Simulation From Tighter Magic Monotones”. [PRX Quantum](#) **2**, 010345 (2021).
- [18] Zi-Wen Liu and Andreas Winter. “Many-body quantum magic”. [PRX Quantum](#) **3**, 020333 (2022).

- [19] Lorenzo Leone, Salvatore F. E. Oliviero, and Alioscia Hamma. “Stabilizer Rényi Entropy”. *Physical Review Letters* **128**, 050402 (2022).
- [20] Shiyu Zhou, Zhicheng Yang, Alioscia Hamma, and Claudio Chamon. “Single T gate in a Clifford circuit drives transition to universal entanglement spectrum statistics”. *SciPost Physics* **9**, 087 (2020).
- [21] Christopher David White, ChunJun Cao, and Brian Swingle. “Conformal field theories are magical”. *Physical Review B* **103**, 075145 (2021).
- [22] Troy J. Sewell and Christopher David White. “Mana and thermalization: Probing the feasibility of near-Clifford Hamiltonian simulation”. *Physical Review B* **106**, 125130 (2022).
- [23] Salvatore F. E. Oliviero, Lorenzo Leone, and Alioscia Hamma. “Magic-state resource theory for the ground state of the transverse-field Ising model”. *Physical Review A* **106**, 042426 (2022).
- [24] Mark Howard and Earl T. Campbell. “Application of a resource theory for magic states to fault-tolerant quantum computing”. *Physical Review Letters* **118**, 090501 (2017).
- [25] James Seddon and Earl Campbell. “Quantifying magic for multi-qubit operations”. *Proceedings of the Royal Society A: Mathematical, Physical and Engineering Sciences* **475**, 20190251 (2019).
- [26] Arne Heimendahl, Felipe Montealegre-Mora, Frank Vallentin, and David Gross. “Stabilizer extent is not multiplicative”. *Quantum* **5**, 400 (2021).
- [27] Hiroki Hamaguchi, Kou Hamada, and Nobuyuki Yoshioka. “Handbook for Efficiently Quantifying Robustness of Magic” (2023). [arxiv:2311.01362](https://arxiv.org/abs/2311.01362).
- [28] SciPy. “`scipy.sparse.csc_matrix`”. *SciPy*.
- [29] Scott Aaronson and Daniel Gottesman. “Improved simulation of stabilizer circuits”. *Physical Review A: Atomic, Molecular, and Optical Physics* **70**, 052328 (2004).
- [30] Mark Howard and Earl Campbell. “Application of a resource theory for magic states to fault-tolerant quantum computing”. *Physical Review Letters* **118**, 090501 (2017).
- [31] Sergey Bravyi, Dan Browne, Padraic Calpin, Earl Campbell, David Gosset, and Mark Howard. “Simulation of quantum circuits by low-rank stabilizer decompositions”. *Quantum* **3**, 181 (2019).
- [32] Stephen Boyd and Lieven Vandenberghe. “Convex optimization”. *Cambridge University Press*. (2004).
- [33] MOSEK ApS. “Mosek modeling cookbook”. *MOSEK* (2019).
- [34] Steven Diamond and Stephen Boyd. “CVXPY: A python-embedded modeling language for convex optimization”. *Journal of Machine Learning Research* **17**, 2909–2913 (2016).
- [35] Akshay Agrawal, Robin Verschueren, Steven Diamond, and Stephen Boyd. “A rewriting system for convex optimization problems”. *Journal of Control and Decision* **5**, 42–60 (2018).
- [36] Reiner Horst and Hoang Tuy. “Branch and bound”. In *Global Optimization: Deterministic Approaches*. Pages 111–172. Springer Berlin Heidelberg (1990).
- [37] G.I. Struchalin, Ya. A. Zagorovskii, E.V. Kovlakov, S.S. Straupe, and S.P. Kulik. “Experimental Estimation of Quantum State Properties from Classical Shadows”. *PRX Quantum* **2**, 010307 (2021).
- [38] Maarten Van den Nest. “Classical simulation of quantum computation, the Gottesman-Knill theorem, and slightly beyond”. *Quantum Inf. Comput.* **10**, 258–271 (2010).

- [39] Jeroen Dehaene and Bart De Moor. “Clifford group, stabilizer states, and linear and quadratic operations over GF(2)”. *Physical Review A* **68**, 042318 (2003).
- [40] Hiroki Hamaguchi, Kou Hamada, and Nobuyuki Yoshioka. “stabilizer\_extent”. [GitHub Repository](#) (2024).
- [41] Guy Desaulniers, Jacques Desrosiers, and Marius M. Solomon Solomon, editors. “Column Generation”. [Springer US](#). (2005).
- [42] Victor Kac and Pokman Cheung. “Quantum Calculus”. [Universitext](#). Springer. (2002).

## A Appendix for Stabilizer Pruning

### A.1 Enumeration of Stabilizer States

In this section, we prove Theorem 1.

**Theorem 1.** *Let  $\mathbb{F}_2$  be the finite field with two elements. For all  $k \in \{1, \dots, n\}$ , we define*

$$\begin{aligned} \mathcal{Q}_k &:= \left\{ Q \mid Q \in \mathbb{F}_2^{k \times k} \text{ is an upper triangular matrix} \right\}, \\ \mathcal{R}_k &:= \left\{ R \mid R \in \mathbb{F}_2^{n \times k} \text{ is a reduced column echelon form matrix with } \text{rank}(R) = k \right\}, \\ \mathcal{T}_R &:= \left\{ t \mid t \in \mathbb{F}_2^n \text{ is a representative of element in the quotient space } \mathbb{F}_2^n / \text{Im}(R) \right\}. \end{aligned}$$

We also define the set of states  $\mathcal{S}_{n,k}$  as

$$\mathcal{S}_{n,k} := \left\{ \frac{1}{2^{k/2}} \sum_{x=0}^{2^k-1} (-1)^{x^\top Q x} i^{c^\top x} |Rx + t\rangle \mid Q \in \mathcal{Q}_k, c \in \mathbb{F}_2^k, R \in \mathcal{R}_k, t \in \mathcal{T}_R \right\}, \quad (4)$$

and define  $\mathcal{S}_{n,0} := \{|t\rangle \mid t \in \mathbb{F}_2^n\}$ . Then, we have  $\bigcup_{k=0}^n \mathcal{S}_{n,k} = \mathcal{S}_n$ .

*Proof.* The main idea comes from Ref. [37]. From previous work [37, Theorem 2][38, Section 5][39, Theorem 5.(ii)], we know that any state in  $\bigcup_{k=0}^n \mathcal{S}_{n,k}$  is a stabilizer state. Thus, we can construct a inclusion map from  $\bigcup_{k=0}^n \mathcal{S}_{n,k}$  to  $\mathcal{S}_n$ . In this proof, we will show that this map is bijective, which means this map is an identity mapping. The assertion is trivial for the case  $k = 0$  with  $2^n$  instances. We will only consider the case  $k > 0$ . Define  $f : (Q, c, R, t) \mapsto |\phi\rangle$  as a map from  $(Q, c, R, t)$  to the corresponding stabilizer state  $|\phi\rangle$ . We will confirm that  $f$  is bijective. Firstly, we show that  $f$  is injective. We can say that

$$\begin{aligned} \left\{ R_1 x + t_1 \mid x \in \mathbb{F}_2^k \right\} &= \left\{ R_2 x + t_2 \mid x \in \mathbb{F}_2^k \right\} \\ \iff (\text{Im}(R_1) = \text{Im}(R_2)) \wedge (t_1 - t_2 \in \text{Im}(R_1)) \\ \iff R_1 = R_2 \wedge t_1 = t_2. \end{aligned}$$

The last equivalence is due to the property of the reduced column echelon form and the quotient space. Given that  $Q$  is an upper triangular matrix, both  $Q$  and  $c$  can be uniquely reconstructed from the amplitude of the state. Consequently, the function  $f$  is injective.

Secondly, we show that  $f$  is surjective. Since  $f$  is injective, we only have to show that the cardinality of the domain is equal to that of the codomain, i.e.,  $-2^n + |\mathcal{S}_n|$ . It is known that the number of  $\mathbb{F}_2^{n \times k}$  reduced column echelon form matrices  $R$  with  $\text{rank}(R) = k$  is

$\begin{bmatrix} n \\ k \end{bmatrix}_2$ , which is a q-binomial coefficient with  $q = 2$  [42, Theorem 7.1]. Therefore, the number of  $Q, c, R, t$  is  $2^{k(k+1)/2}, 2^k, \begin{bmatrix} n \\ k \end{bmatrix}_2, 2^{n-k}$ , respectively. The total number of states is

$$\sum_{k=1}^n 2^{k(k+1)/2} 2^k \begin{bmatrix} n \\ k \end{bmatrix}_2 2^{n-k} = -2^n + 2^n \sum_{k=0}^n \begin{bmatrix} n \\ k \end{bmatrix}_2 2^{k(k+1)/2} = -2^n + 2^n \prod_{k=1}^n (2^k + 1) = -2^n + |\mathcal{S}_n|.$$

In the second to last equation, we used the q-binomial theorem. Therefore, the mapping is surjective, which completes the proof.  $\square$

## A.2 Pruning for the Branch and Bound Method

In Section 3.1, we explained the branching in the branch and bound method. This algorithm can be much faster by the bounding introduced in this section. Firstly, recall that we are maximizing the following:

$$\max_{Q,c} \left\{ \left| \sum_{x=0}^{2^n-1} (-1)^{x^\top Qx} i^{c^\top x} P_x \right| \right\}.$$

This can be easily bounded by

$$\max_{Q,c} \left\{ \left| \sum_{x=0}^{2^n-1} (-1)^{x^\top Qx} i^{c^\top x} P_x \right| \right\} \leq \max_{Q,c} \left\{ \sum_{x=0}^{2^n-1} \left| (-1)^{x^\top Qx} i^{c^\top x} P_x \right| \right\} = \sum_{x=0}^{2^n-1} |P_x|.$$

Such a bound is crucial for the branch and bound method, because it allows us to terminate the branch if the bound is inferior to the current best value. However, the bound can be more refined. Since each coefficient takes only 1,  $-1, i$  or  $-i$ , we can bound as

$$\max_{Q,c} \left\{ \left| \sum_{x=0}^{2^n-1} (-1)^{x^\top Qx} i^{c^\top x} P_x \right| \right\} \leq \max_{c_x} \left\{ \left| \sum_{x=0}^{2^n-1} i^{c_x} P_x \right| \right\}, \quad (7)$$

where  $c_x$  takes values independently from the set  $\{0, 1, 2, 3\}$ . Let  $P := \sum_{x=0}^{2^n-1} i^{c_x} P_x$ , and define  $\theta_x := \arg(i^{c_x} P_x)$ . The value  $\max_{c_x} \{|P|\}$  is equals to

$$\max_{c_x, \theta} \left\{ \langle P, e^{i\theta} \rangle \right\} = \max_{c_x, \theta} \left\{ \sum_{x=0}^{2^n-1} \langle i^{c_x} P_x, e^{i\theta} \rangle \right\} = \max_{c_x, \theta} \left\{ \sum_{x=0}^{2^n-1} |P_x| \cos(\theta_x - \theta) \right\} \quad (8)$$

where  $\langle \cdot, \cdot \rangle$  denotes the inner product of complex values. Then, we can confirm that Algorithm 2 is certain to return the optimal solution for (7) as follows. If we fix the value of  $\theta$  in (8), the optimal values of  $c_x$  can be determined so that  $\cos(\theta_x - \theta)$  is maximized, i.e.,  $\theta_x \in [\theta - \pi/4, \theta + \pi/4)$ . Thus, instead of trying all  $\theta$ , we run Algorithm 2 to cover all the possible optimal solutions of  $c_x$ , which is sufficient to calculate  $\max_{c_x} \{|P|\}$ .

Refer to Fig. 4 for a visual representation of this algorithm. The time complexity of this approach is  $\mathcal{O}(n2^n)$  owing to the sorting of  $2^n$  elements.

As the end of this section, we evaluate the performance of this bound. We can obtain the lower bound of (8) by taking the expected value with respect to  $\theta$  as follows:

$$\begin{aligned} \max_{c_x} \{|P|\} &= \max_{c_x, \theta} \left\{ \sum_{x=0}^{2^n-1} |P_x| \cos(\theta_x - \theta) \right\} \\ &\geq \mathbb{E} \left[ \max_{c_x} \left\{ \sum_{x=0}^{2^n-1} |P_x| \cos(\theta_x - \theta) \right\} \right] = \sum_{x=0}^{2^n-1} |P_x| \cdot \mathbb{E} \left[ \max_{c_x} \{ \cos(\theta_x - \theta) \} \right]. \end{aligned} \quad (9)$$

---

**Algorithm 2:** Bounding for the Branch and Bound Method
 

---

**Input:** Coefficients  $P_x$  for  $x = 0, 1, \dots, 2^n - 1$ 
**Output:** The answer for problem (7)

- 1 Take  $c_x$  that satisfies  $\theta_x \in [0, \pi/2)$
  - 2 Sort and relabel  $P_x$  so that  $0 \leq \theta_0 \leq \theta_1 \leq \dots \leq \theta_{2^n-1} < \pi/2$ .
  - 3  $\text{ans} \leftarrow 0$
  - 4 **for**  $x \leftarrow 0$  **to**  $2^n - 1$  **do**
  - 5      $\text{ans} \leftarrow \max\left(\text{ans}, \left|\sum_{x=0}^{2^n-1} i^{c_x} P_x\right|\right)$
  - 6      $c_x \leftarrow c_x + 1$
  - 7 **return**  $\text{ans}$
- 

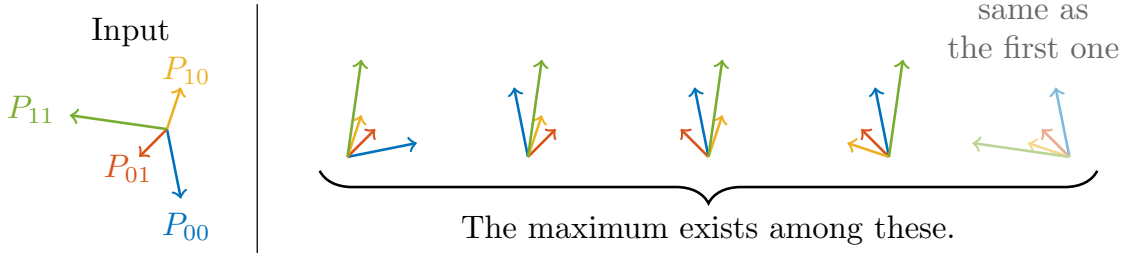


Figure 4: Visualization of Algorithm 2. Suppose that  $n = 2$  and  $P_x$  are represented as the vectors in the complex plane (e.g.,  $P_{00} = 1 - 5i$ ) on the left side. Iterating the loop in Algorithm 2 yields  $2^n$  patterns of the coefficients  $c_x$ , as depicted on the right side. The maximum of problem (7) exists among these  $2^n$  patterns.

Here, we assume  $\theta$  is drawn from the uniform distribution over  $[0, 2\pi)$ . Then, we can replace each term  $\mathbb{E}[\max_{c_x} \{\cos(\theta_x - \theta)\}]$  with  $\mathbb{E}[\cos(\theta'_x)]$  where  $\theta'_x$  follows the uniform distribution over the interval  $[-\pi/4, +\pi/4)$ . Then, we can derive that

$$\frac{\max_{c_x} \{|P|\}}{\sum_{x=0}^{2^n-1} |P_x|} \geq \frac{\sum_{x=0}^{2^n-1} |P_x| \cdot \mathbb{E}[\cos \theta'_x]}{\sum_{x=0}^{2^n-1} |P_x|} = \frac{\int_{-\pi/4}^{+\pi/4} \cos(\theta) d\theta}{\pi/2} = \frac{2\sqrt{2}}{\pi} = 0.900316 \dots$$

The result of a numerical experiment suggests that this lower bound serves as a rough approximation of the ratio. We independently sampled  $P_x$  from the standard normal distribution and  $\theta_x$  from the uniform distribution over  $[0, 2\pi)$ . The numerical experiment results obtained are as follows. Firstly, the average of

$$\frac{\max_{c_x} \{|P|\}}{\sum_{x=0}^{2^n-1} |P_x|} = \frac{\max_{c_x} \left\{ \left| \sum_{x=0}^{2^n-1} i^{c_x} P_x \right| \right\}}{\sum_{x=0}^{2^n-1} |P_x|}$$

over 100 runs yielded 0.935624 for  $n = 4$ . This confirms that Algorithm 2 provides a better bound compared to  $\sum_{x=0}^{2^n-1} |P_x|$ . However, in the same setting, it turned out that the average of

$$\frac{\max_{Q,c} \left\{ \left| \sum_{x=0}^{2^n-1} (-1)^{x^\top Q} i^{c^\top x} P_x \right| \right\}}{\sum_{x=0}^{2^n-1} |P_x|}$$

yielded 0.824056, implying the bound (7) may not necessarily be optimal. Whether a better bound can be obtained with fewer computational cost is left for an open problem.